Large-Area Fabrication of Droplet Pancake Bouncing Surface and Control of Bouncing State

Jinlong Song[1,2], Mingqian Gao[1,2], Changlin Zhao[1,2], Yao Lu[3], Liu Huang[1,2], Xin Liu[1,2], Claire, J. Carmalt[4], Xu Deng[5], Ivan P. Parkin[4]*

[1]Key Laboratory for Precision and Non-traditional Machining Technology of the Ministry of Education, Dalian University of Technology, Dalian 116024, P. R. China.

[2]Collaborative Innovation Center of Major Machine Manufacturing in Liaoning, Dalian University of Technology, Dalian 116024, China.

[3]Nanoengineered Systems Laboratory, UCL Mechanical Engineering, University College London, London, WC1E 7JE, UK.

[4]Department of Chemistry, University College London, 20 Gordon Street, London, WC1H 0AJ, UK.

[5]Institute of Fundamental and Frontier Sciences, University of Electronic Science and Technology of China, Chengdu 610054, P. R. China.

*Email: xinliu@dlut.edu.cn.

KEYWORDS: pancake bouncing, superhydrophobic, pillar arrays, millimeter diameter, large-area

ABSTRACT: Superhydrophobic pillar arrays, which can generate the droplet pancake bouncing phenomenon with reduced liquid-solid contact time, have huge application prospects in anti-icing of aircraft wings from freezing rain. However, the previously reported pillar arrays, suitable to obtain pancake bouncing, have diameter ≤ 100 μm and height-diameter-ratio > 10, which are difficult to fabricate over a large-area. Here, we have systematically studied the influence of the dimension of the superhydrophobic pillar arrays on the bouncing dynamics of water droplets. We show that the typical pancake bouncing with 57.8% reduction in contact time with the surface was observed on the superhydrophobic pillar arrays with 1.05 mm diameter, 0.8 mm height and 0.25 mm space. Such pillar arrays with millimeter diameter and < 1 height-diameter-ratio can be easily fabricated over large areas. Further, a simple replication-spraying method was developed for the large-area fabrication of the superhydrophobic pillar arrays to induce pancake bouncing. No sacrificial layer was needed to reduce the adhesion in the replication processes. Since the bouncing dynamics were rather sensitive to the space between the pillars, a method to control the contact time, bouncing shape, horizontal bouncing direction and reversible switch between pancake bouncing and conventional bouncing was realized by adjusting the inclination angle of the shape memory polymer pillars.

Controlling droplet dynamics on various wettability and textured surfaces has been widely studied because of its potential application prospect in pesticide sprays,[1] self-cleaning,[2,3] and anti-icing.[4] Water droplets impacting on a waterproof (*e.g.* superhydrophobic) surface often bounce and leave the substrate.[5-13] The recent research focus on controlling the droplet dynamics on waterproof surface can be classified into two categories: one is increasing the liquid-solid contact time and another is decreasing the liquid-solid contact time.[1,14-16] Compared with increasing the contact time, decreasing the contact time on waterproof surfaces has fascinated

more scientists because of its greater industrial application potential in, for example, anti-icing of aircraft wings and protecting high voltage transmission lines from freezing rain.

A water droplet impacting on a superhydrophobic flat surface often spreads first, then recoils and finally completely leaves the surface. The contact time of a water droplet on a superhydrophobic surface is independent of the impact velocities but depends on the volume of water droplet, which means the contact time is constant for a certain volume of water droplet.[17] However, very recently, researchers observed that the contact time was also affected by the surface texture and under ideal conditions, a rapid droplet detachment was promoted and realized. Bird *et al.* reduced the contact time by adding a superhydrophobic microscope ridge with height of ~180 μm on the superhydrophobic flat surfaces.[18] When water droplets impacted on the ridge at high enough impact velocity, the droplet broke up and split into smaller ones, which redistributed the volume and altered the droplet hydrodynamics. The overall contact time was reduced by ~37% compared with that in the non-splitting condition. Gauthier *et al.* further studied the influence of microscope ridge size, impact velocity, and droplet volume on bouncing dynamics.[19] The contact time showed a step-like variation with impact velocity and was reduced by ~44% without splitting. Liu *et al.* studied the droplet impinging on the macroscopic cylindrically curved surfaces.[20] The water droplet impinging on cylindrical convex surfaces exhibited symmetry breaking and asymmetric bouncing dynamics with a contact time reduction of ~40%. Although the aforementioned surface textures can reduce the contact time effectively, it is not suitable for practical applications, for example, most rain droplets will not touch a single strip-like texture. In 2014, Liu *et al.* observed pancake bouncing on the superhydrophobic submillimeter-scale pillar arrays with the contact time reduced by ~80%.[21,22] This pillar arrays can ensure that all water droplets touch the surface texture and quickly detach from the substrate.

This makes these surfaces suitable for practical applications, such as anti-icing of aircraft wings in the freezing rain environments. The pillar diameter and height designed by Liu were 20~100 μm and 800~1200 μm, respectively, which was fabricated by electric spark cutting. However, the processing efficiency of electric spark cutting for those pillar arrays was rather low,[23] furthermore the pillar arrays with such small diameter and large height-diameter-ratio were also difficult for large-area fabrication by using traditional or nontraditional processing methods.

Mold replication technology, including casting and thermal extrusion, is widely considered as one of the most effective methods to fabricate large-area superhydrophobic surfaces because of its high efficiency, low cost, and easy operation.[24-28] However, it is very difficult to lift the replicated pillar arrays with diameter <100 μm and height-diameter-ratio >10 off from the mold even when using perfluoro monolayer and water-soluble sacrificial layer to reduce the adhesion between the replica and the mold.[29] Here, we explored if pancake bouncing of water droplet can occur on the pillar arrays with a larger diameter and smaller height-diameter-ratio by adjusting the dimension of the superhydrophobic pillar arrays. We were surprised to find that the typical pancake bouncing with a 57.8% reduction in contact time was observed on the superhydrophobic pillar arrays with 1.05 mm diameter and 0.8 mm height. Pillar arrays with such large diameter and small height-diameter-ratio can be easily and completely lifted off from the mold without any adhesion-reduction modification. Based on this, we then developed a simple replication-spraying method to realize the large-area fabrication of the superhydrophobic pillar arrays. In the dimension optimization process, we found that the contact time was rather sensitive to the space between the pillars. Combined with a shape memory polymer (SMP), the control of the contact time, bouncing shape, horizontal bouncing direction, and the reversible switch between pancake

bouncing and conventional bouncing was achieved by adjusting the inclination angle of pillars which also adjusting the space.

RESULTS AND DISCUSSION

Dimension optimization of superhydrophobic pillar arrays for pancake bouncing

Figure 1(a) and 1(b) show the SEM images of the superhydrophobic flat surface composed of a glass slide surface coated with *Never Wet* nano-coatings. On this surface, the impacting water droplet (volume V = 17.9 μL, radius r_0 = 1.62 mm, We = 13.3) spread to a uniform thin film, retracted and then detached from the surface with total liquid-solid contact time of 21.4 ms, showing a conventional bouncing phenomenon (Figure 1(c) and Video S1). Figure 1(d) and 1(e) shows the SEM images of the superhydrophobic pillar arrays (diameter D = 0.3 mm, space S = 0.2 mm and height H = 1 mm, Figure S1). On this surface, water droplet spread laterally along the horizontal direction and penetrated longitudinally into the space between the pillars but finally detached from the surface as pancake bouncing with Q of 0.98 and total liquid-solid contact time of 7.9 ms (Figure 1(f) and Video S2). The formation mechanism of the pancake bouncing on the superhydrophobic pillar arrays is that the kinetic energy of a water droplet is stored as surface energy during the downward processes and then surface energy is converted back into kinetic energy to push the droplet back out of the surface during the upward processes in the whole liquid-solid contact processes.[21,22,30,31] Although the superhydrophobic pillar arrays for pancake bouncing with short liquid-solid contact time has application prospects in anti-icing, self-cleaning, and stay-drying, the pillars with small diameter and large height-diameter-ratio are difficult to be large-area fabricated, seriously hindering the practical applications of the pancake bouncing surfaces. Thus, the dimension of the superhydrophobic pillar arrays for pancake bouncing need to be optimized to be suitable for large-area fabrication.

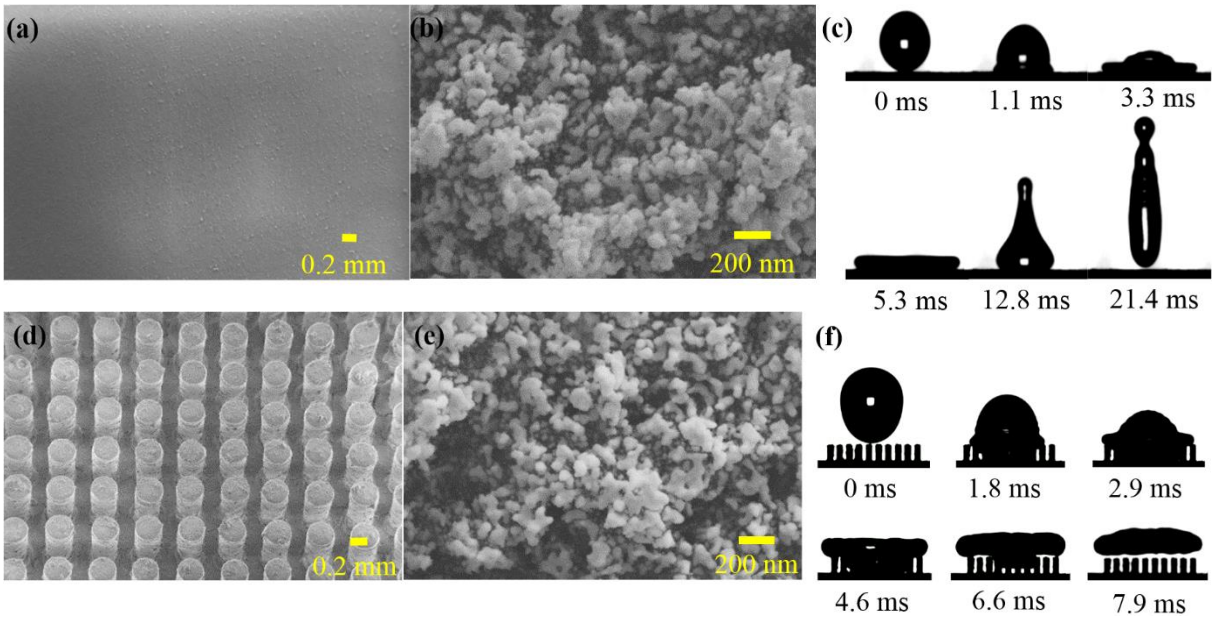

Figure 1. Different bouncing phenomenon of water droplets on the superhydrophobic flat surface and superhydrophobic pillar arrays. (a)-(b) SEM images of the superhydrophobic flat surfaces with different magnifications. (c) Selected snapshots captured by high-speed camera showing a water droplet (17.9 μL, r_0 = 1.62 mm) impacting on the superhydrophobic flat surface at *We* = 13.3. (d)-(e) SEM images of the superhydrophobic pillar arrays with *D* = 0.3 mm, *S* = 0.2 mm, and *H* = 1 mm with different magnifications. (f) Selected snapshots captured by the high-speed camera showing a water droplet (17.9 μL, r_0 = 1.62 mm) impacting on the superhydrophobic pillar arrays at *We* = 13.3.

We next studied the influence of dimension of the superhydrophobic pillar arrays on the contact time $t_{contact}$ and *Q*. The pillar height was kept constant at 1 mm for the storage of adequate capillary energy.[21] The volume of water droplet used in here was 17.9 μL. In order to fabricate the mold more easily and the replicated pillars could be lifted off completely, the diameter and space between the pillars should be as large as possible. Figure 2(a) shows the variations of the contact time and *Q* with the space *S* between the pillars (*D* = 0.3 mm, *H* = 1 mm) at *We* = 13.3.

The contact time $t_{contact}$ increased with the space while the Q decreased with the space between the pillars. $Q > 0.8$ occurred on the pillars with S = 0.2 mm and 0.25 mm, whereas it was absent on the pillars with S = 0.3 mm and 0.4 mm. Thus, the largest space to form pancake bouncing is about 0.25 mm, where the water droplet shows a pancake bouncing with $Q \sim 0.93$ and $t_{contact} \sim$ 8.8 ms, as shown in Figure 2(b). Then, the space was constant at 0.25 mm and the effect of the pillar diameter was studied. Figure 2(c), 2(d) and Figure S2 show the variations of the contact time and Q with the diameter D (S = 0.25 mm and H = 1mm) at We = 13.3. We were surprised to find that within D = 1.25 mm, $t_{contact}$ was smaller than 9 ms and Q was larger than 0.88, showing typical pancake bouncing. However, for D = 1.55 mm, the water droplet exhibits a conventional complete rebound with $Q \sim 0.39$ and $t_{contact} \sim 19.9$ ms. Thus, for water droplet with volume of 17.9 μL, the largest diameter to form pancake bouncing is 1.25 mm, in that diameter, the water droplet shows a pancake bouncing with $Q \sim 0.88$ and $t_{contact} \sim 8.9$ ms. Figure 2(e)-2(g) shows the SEM images of the superhydrophobic pillar arrays with D = 1.15 mm, S = 0.25 mm, and H = 1 mm, the water droplet impacting on it shows a pancake bouncing with $Q \sim 0.98$ and $t_{contact} \sim 8.3$ ms, also as shown in Video S3.

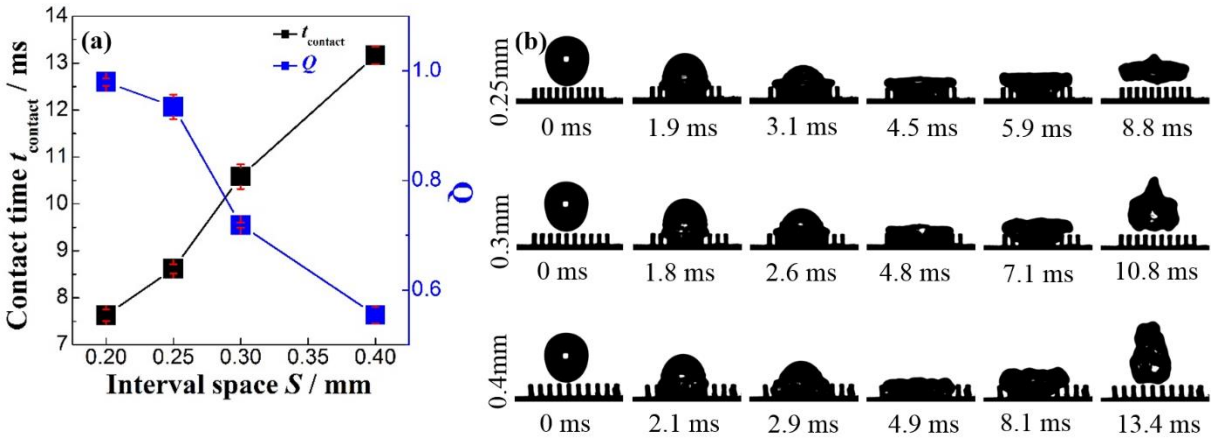

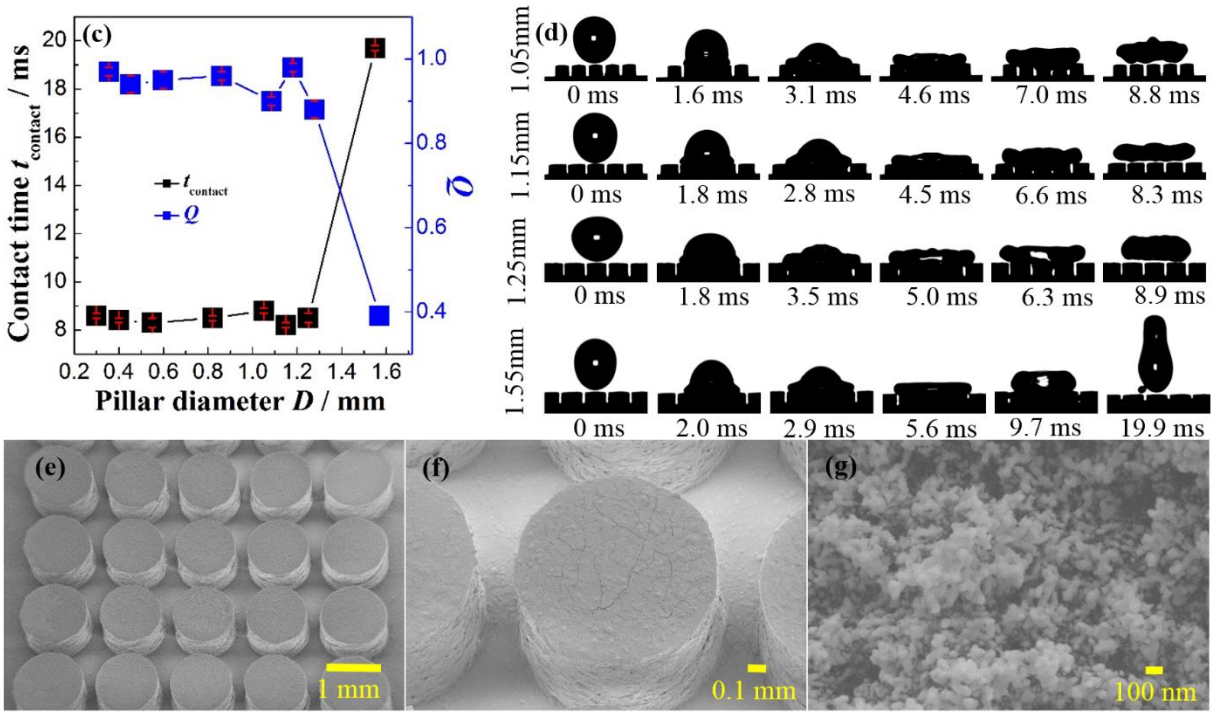

Figure 2. The influence of dimension on the liquid-solid contact time and bouncing shape. (a) The variations of the contact time $t_{contact}$ and Q of a water droplet (17.9 μL, r_0 = 1.62) with the space between the pillars (D = 0.3 mm and H = 1 mm) at We = 13.3. (b) Selected snapshots captured by the high-speed camera showing a water droplet (17.9 μL, r_0 = 1.62 mm) impacting on the superhydrophobic pillar arrays with different space between the pillars (D = 0.3mm and H = 1 mm) at We = 13.3. (c) The variations of the contact time and Q with the pillar diameter (S = 0.25 mm and H = 1 mm) at We = 13.3. (d) Selected snapshots captured by a high-speed camera showing a water droplet (17.9 μL, r_0 = 1.62 mm) impacting on the superhydrophobic pillar arrays with different pillar diameters (S = 0.25 mm and H = 1 mm) at We = 13.3. (e)-(g) SEM images of the superhydrophobic pillar arrays with different magnifications (D = 1.15 mm, S = 0.25 mm, and H = 1 mm). The water droplet impacting on it showed a pancake bouncing with Q～0.98 and $t_{contact}$～8.3 ms.

We also studied the influence of *We* on the contact time and *Q* and tried to find the critical smallest *We* for pancake bouncing. Figure 3 shows the variation of the contact time $t_{contact}$ and *Q* of a water droplet (17.9 μL, r_0 = 1.62) with *We* on the superhydrophobic pillar arrays with different diameters. The space and height of the pillars were constant at 0.25 mm and 1 mm, respectively. For *D* = 1.55 mm, no pancake bouncing appeared at any *We*. For *D* = 1.25 mm and 1.15 mm, pancake bouncing appeared at *We* ≥ 12.8 and *We* ≥ 8.8, respectively. When D ≤ 1.05 mm, the critical *We* to realize pancake bouncing was constant at 5.5 that is pancake bouncing appeared at *We* ≥ 5.5. The aforementioned results indicate that when *D* ≤ 1.05 mm, pancake bouncing can be obtained at the largest region of *We*.

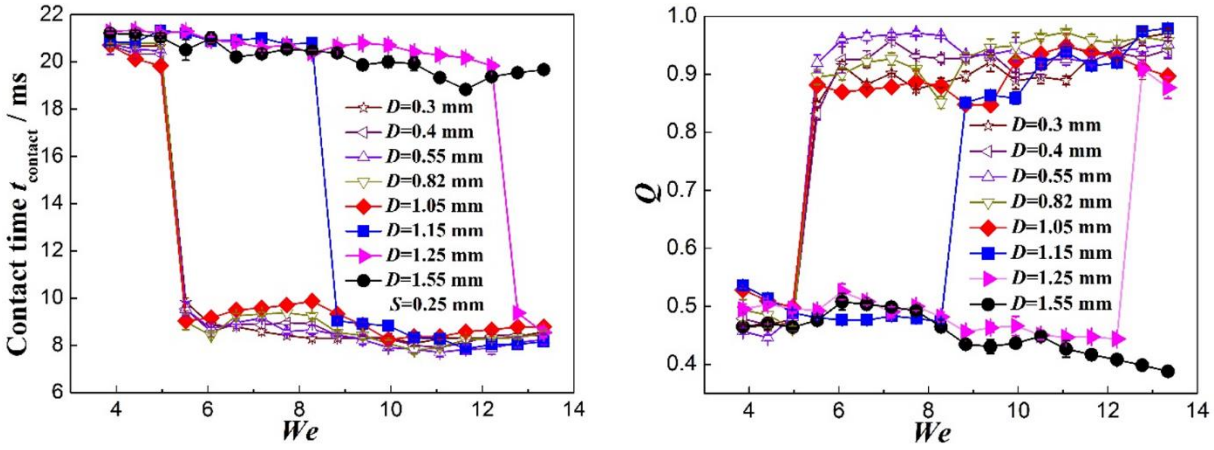

Figure 3. The variation of the contact time $t_{contact}$ (a) and *Q* (b) of a water droplet (17.9 μL, r_0 = 1.62) with *We* on the superhydrophobic pillar arrays with different diameters (*S* = 0.25 mm and *H* = 1 mm).

For the superhydrophobic pillar arrays with small diameter, Liu *et al.* pointed out that pancake bouncing is rather insensitive to the pillar height.[21] In their experiment, for *D* = 0.1 mm, *H* from 0.5 mm to 1.2 mm is feasible for pancake bouncing. The similar law was found for large diameters studied here. Figure 4(a) shows the variation of the contact time $t_{contact}$ and *Q* of a water droplet (17.9 μL, r_0 = 1.62) on the superhydrophobic pillar arrays with different height *H*

(D = 1.05 mm and S = 0.25 mm) at We = 13.3. The pancake bouncing was present at H = 0.6 mm to 1.0 mm, for the height H > 1.0 mm and < 0.6 mm, conventional bouncing was present, as shown in Figure 4(b).

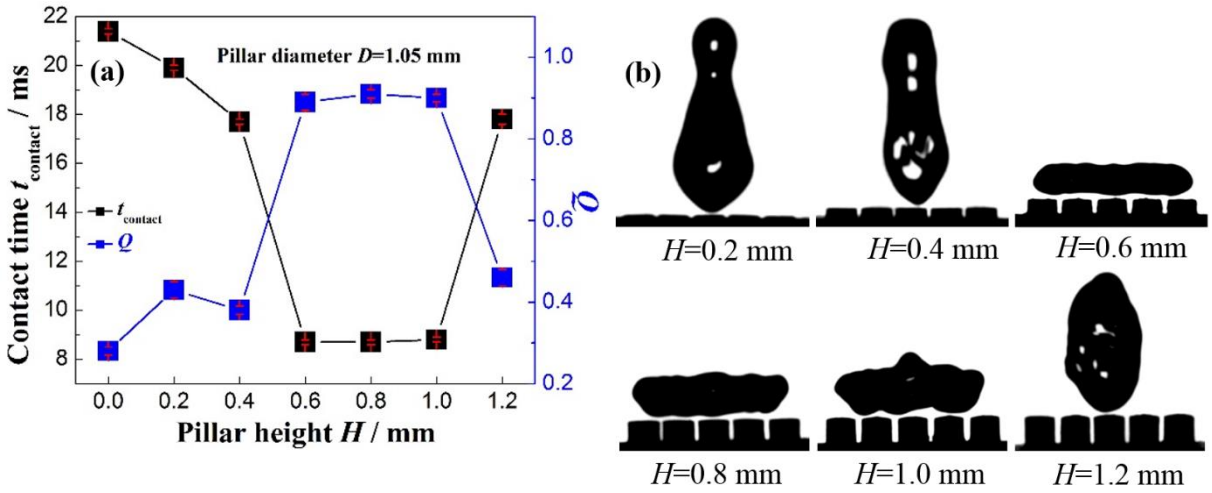

Figure 4. The variation of the contact time $t_{contact}$ and Q of a water droplet (17.9 μL, r_0 = 1.62) on the superhydrophobic pillar arrays with different height H (D = 1.05 mm and S = 0.25 mm) at We = 13.3 (a) and the detachment moment of the water droplet on the superhydrophobic pillar arrays (b).

We also studied the influence of the volume of water droplet on the bouncing shape. Figure 5(a) and Figure S3 show the variation of Q and droplet shape at the detachment moment with the droplet volume on the superhydrophobic pillar arrays with D = 1.05 mm and S = 0.25 mm at We=13.3. The water droplets with volume ≥ 13.9 μL shows the pancake bouncing with Q > 0.8. However, the conventional bouncing was present for water droplets with volume < 13.9 μL, which means the water droplets with volume < 13.9 μL cannot obtain pancake bouncing on the superhydrophobic pillar arrays with D = 1.05 mm and S = 0.25 mm. Obviously, the pancake bouncing is affected by the droplet volume. Then, we studied the critical pillar diameter suitable to obtain pancake bouncing for water droplet with different volume. Figure 5(b) shows the

variation of Q with the diameter D (S = 0.25 mm and H = 1 mm) for different droplet volume. We found that the largest diameter to form pancake bouncing increased with the increase of the droplet volume. The largest diameter to form pancake bouncing for 7.9 μL, 11 μL, 13.9 μL, and 17.9 μL water droplet are 0.55 mm, 0.82 mm, 1.05 mm, and 1.25 mm, respectively.

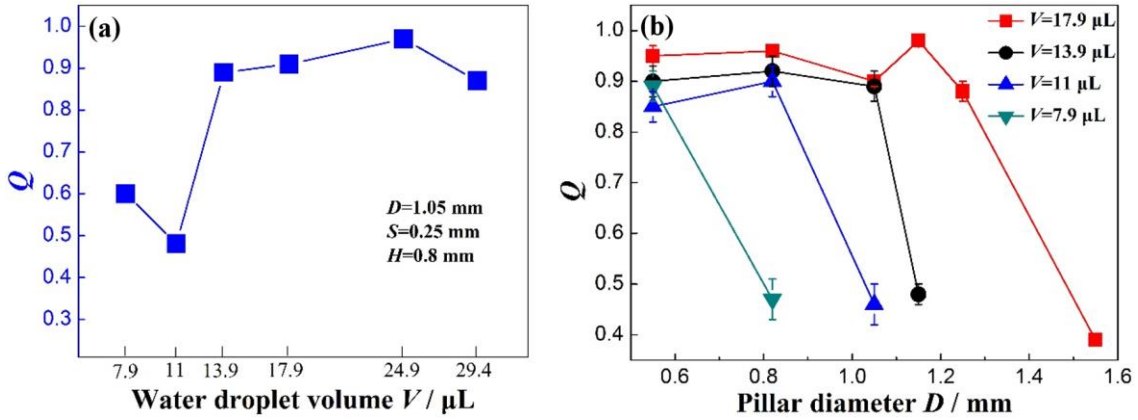

Figure 5 The influence of water droplet volume on Q. (a) The variation of Q with the droplet volume on the superhydrophobic pillar arrays with D = 1.05 mm, S = 0.25 mm, and H = 0.8mm at We=13.3. (b) The variation of Q with the diameter D (S = 0.25 mm and H = 1 mm) of the superhydrophobic pillar arrays for different droplet volume at We=13.3.

Since one of the important application prospects of the droplet pancake bouncing surface is anti-icing, we tested the bouncing phenomenon of cold water droplet on the superhydrophobic pillar arrays. Figure S4 shows the bouncing processes of water droplets with temperature of 1 °C and 5 °C on the superhydrophobic pillar arrays with D = 1.05 mm, S = 0.25 mm, and H= 0.8 mm at We=13.3. The droplets shows a typical pancake bouncing with $t_{contact}$～8.5 ms, indicating possible application in the freezing environment.

Large-area fabrication of superhydrophobic pillar arrays

Since the height-diameter-ratio of the superhydrophobic pillar arrays for pancake bouncing can be smaller than 1 and the diameter of the pillar arrays can be larger than 1 mm, these kinds of pillars can be easily replicated and lifted off completely from the mold without any damage to the mold. We developed two kinds of replication methods, casting and thermal extrusion, to fabricate the superhydrophobic pillar arrays. Figure 6(a)-6(f) shows the schematics of the fabrication processes of the superhydrophobic pillar arrays by casting-replication. The blind hole arrays with diameter of 1.05 mm, space of 0.25 mm, and depth of 0.8 mm on Al substrates were used as mold and polydimethylsiloxane (PDMS, Sylgard 184, Dow Corn-ing, Germany) as the representative casting body. The PDMS:cross-linker ratio was 10:1. After curing, the PDMS pillars were lifted off easily by hand. After coating with the superhydrophobic nano coatings, the PDMS superdrophobic pillar arrays with D = 1.05 mm, S = 0.25 mm, and H = 0.8 mm were obtained. The water droplet with We=13.3 on the PDMS superhydrophobic pillar arrays shows pancake bouncing with $t_{contact}$ = 8.6 ms and Q = 0.87. Figure 6(g)-6(l) shows the schematics of the fabrication processes of the superhydrophobic pillar arrays by extrusion-replication. The through hole arrays with diameter of 1.05 mm, space of 0.25 mm, and depth of 0.8 mm on Al substrates were used as a mold and polypropylene (PP) as the representative thermal extrusion body. For the polymer, when the substrate temperature is higher than the thermal deformation temperature of that polymer, the extrusion formation of polymer was easily realized. After thermal extrusion, the PP pillars were also shown to lift off easily by hand. After coating with the superhydrophobic nano coatings, the PP superhydrophobic pillar arrays with D = 1.05 mm, S = 0.25 mm, and H = 0.8 mm were obtained. The water droplet with We = 13.3 on the PP superhydrophobic pillar arrays shows pancake bouncing with $t_{contact}$ = 9 ms and Q = 0.88.

Therefore, the dimension optimized superhydrophobic pillar arrays for pancake bouncing can be easily and economically large-area fabricated on polymer substrate, which could promote the practical application of the water droplet pancake bouncing surface. It's also worth noting that no sacrificial layer was needed to reduce the adhesion in the replication processes because of small height-diameter-ratio. Figure 6(m), 6(n), Figure S5, and Video S4 show the large-area mold and large-area water droplet pancake bouncing surface with size of 150 mm × 100 mm × 20 mm which was obtained by extrusion-replication-spraying. The replication-spraying method can also be easily extended to the large-area fabrication of the metal superhydrophobic pillar arrays.

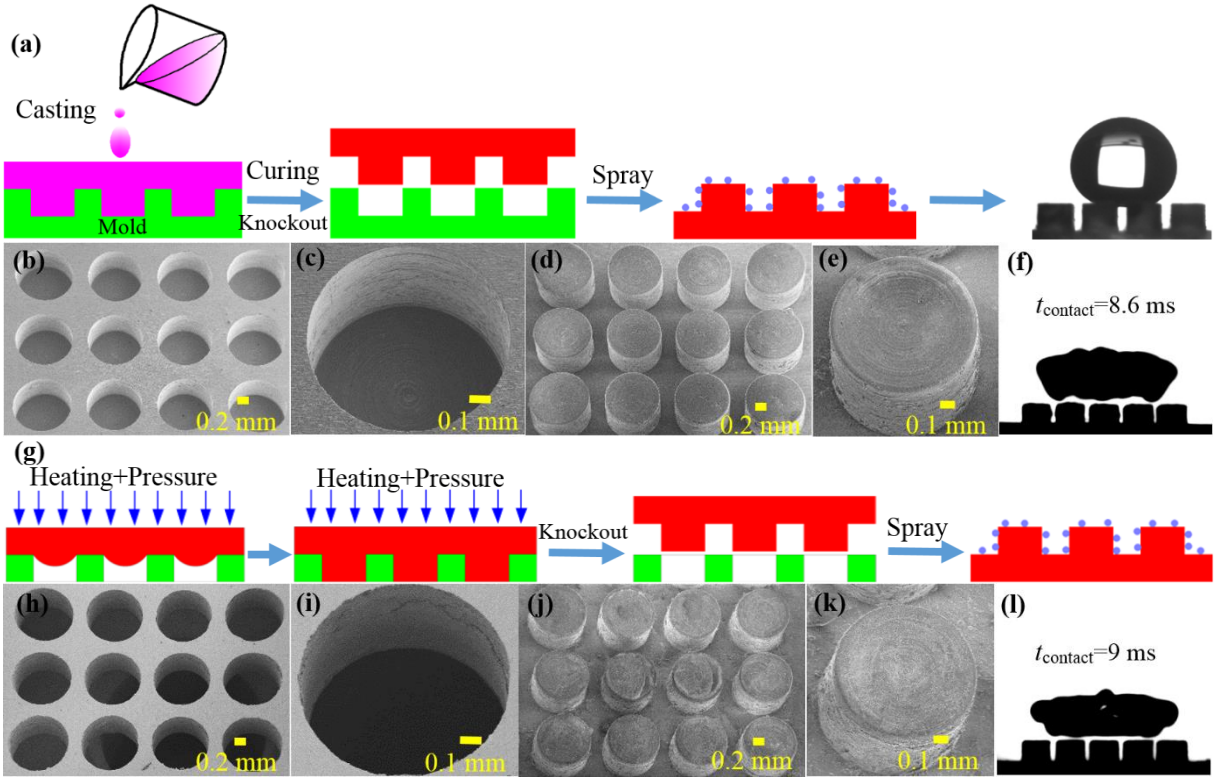

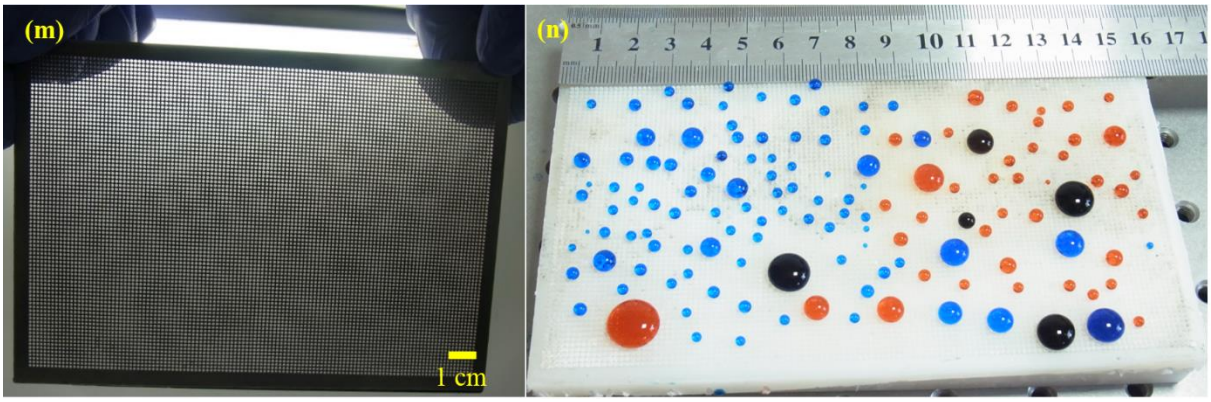

Figure 6. Fabrication of the superhydrophobic pillar arrays for pancake bouncing by replication-spraying. (a) Schematics of the fabrication processes of the superhydrophobic pillar arrays by casting-replication. The blind hole arrays was used as mold. (b)-(c) SEM images of the blind hole arrays with different magnifications on Al substrate obtained by drilling. (d)-(e) SEM images of the replicated PDMS superhydrophobic pillar arrays with different magnifications. (f) The replicated PDMS superhydrophobic pillar arrays show pancake bouncing with $t_{contact}$ = 8.75 ms and Q = 0.97. (g) Schematics of the fabrication processes of the superhydrophobic pillar arrays formed by extrusion-replication. The through hole arrays were used as a mold. (h)-(i) SEM images of the through hole arrays with different magnifications on Al substrate obtained by drilling. (j)-(k) SEM images of the replicated PP superhydrophobic pillar arrays with different magnifications. (l) The replicated PP superhydrophobic pillar arrays show pancake bouncing with $t_{contact}$ = 9 ms and Q = 0.98. The inner pore diameter of the Al mold is 1.05 mm and the outside pillar diameter of the replicated PDMS and PP pillars is about 1.05 mm. (m) Digital photo of the large-area mold with through hole arrays with D = 1.05 mm, S = 0.25 mm, and H = 0.8 mm. The size of the mold is 150 mm × 100 mm × 20 mm. (n) Digital photo of the large-area PP superhydrophobic pillar arrays with D = 1.05 mm, S = 0.25 mm, and H = 0.8 mm for pancake bouncing obtained by extrusion-replication-spraying. The size of the PP plate is 150 mm × 100

mm × 20 mm. No sacrificial layer was needed to reduce the adhesion in the replication processes because of the relatively large diameter and small height-diameter-ratio.

Control of bouncing state

In the dimension optimization process, we found that the contact time was sensitive to the space between the pillars, as shown in Figure 2(a) and 2(b). For the superhydrophobic pillars, when the pillars are pressed aslant, the space will change with the inclination angle α, as shown in Figure 7(a). Thus, we experimentally explored if we can control the liquid-solid contact time and bouncing shape at the detachment moment by adjusting the inclination angle. The superhydrophobic pillar arrays composed of the shape memory polymer (SMP) with D = 0.4 mm, H = 1 mm, and S = 0.4 mm were used as substrate. The SMP pillars were easily pressed aslant for different inclination angle under heating condition and different bouncing shape and contact time were obtained, as shown in Figure 7(b) to 7(e) and Video S5. Pancake bouncing was present at α = 32° and 42°, for other bigger or smaller α, the conventional bouncing phenomenon was observed. According to Figure 7(a), the spaces S_1 and S_2 after press are as follows,

$$S_1 = S \cdot \sin\alpha \tag{1}$$

$$S_2 = H \cdot \sin\alpha \cdot \cos\left[\arctan\frac{\sin(\alpha+\arctan\frac{D}{H})}{\frac{D}{\sqrt{D^2+H^2}}+\cos(\alpha+\arctan\frac{D}{H})}\right] - (H\cdot\cos\alpha - S)\cdot\sin\left[\arctan\frac{\sin(\alpha+\arctan\frac{D}{H})}{\frac{D}{\sqrt{D^2+H^2}}+\cos(\alpha+\arctan\frac{D}{H})}\right] \tag{2}$$

Where D = 0.4 mm, H = 1 mm, and S = 0.4 mm, then

$$S_2 = \cos\beta[\sin\alpha - \tan\beta(\cos\alpha - 0.4)] \tag{3}$$

$$\tan\beta = \frac{1.077\sin(21.8°+\alpha)}{0.4+1.077\cos(21.8°+\alpha)} \tag{4}$$

According to Equation (1), (3) and (4), for α = 32° and 42°, (S_1, S_2) are (0.21 mm, 0.12 mm) and (0.27 mm, 0.20 mm), respectively, and pancake bouncing was observed. For α = 54°, (S_1, S_2) is (0.32 mm, 0.28mm), no pancake bouncing was seen. The space suitable to induce pancake bouncing is in good agreement with Figure 2(a). Therefore, the contact time and bouncing shape at the detachment moment can be controlled by adjusting the inclination angle. The relationship between $t_{contact}$, S_1, S_2 with α is shown in Figure 7(f). In addition, we found the horizontal bouncing direction of a water droplet also can be controlled by adjusting the inclination angles of the pillars, as shown in Figure S6. For α = 90°, droplet impacted and rebounded vertically. For α = 66°, 54°, and 42°, droplet impacted and rebounded with some rebound angle and horizontal deviation. For α = 32°, droplet impacted and rebounded vertically again. Based on the special memory ability,[32,33] the pressed and inclined pillars were shortly recovered into the straight pillars after heating, as shown in Figure 7(g) and Figure S7, which guarantees the reversible switching of the bouncing shape, contact time and horizontal bouncing direction, as shown in Figure 7(h).

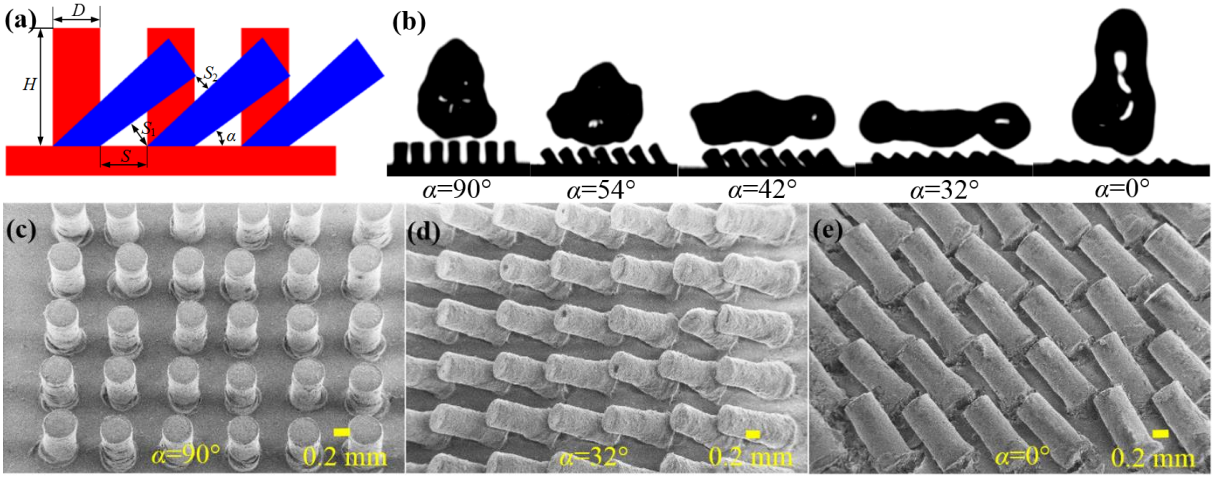

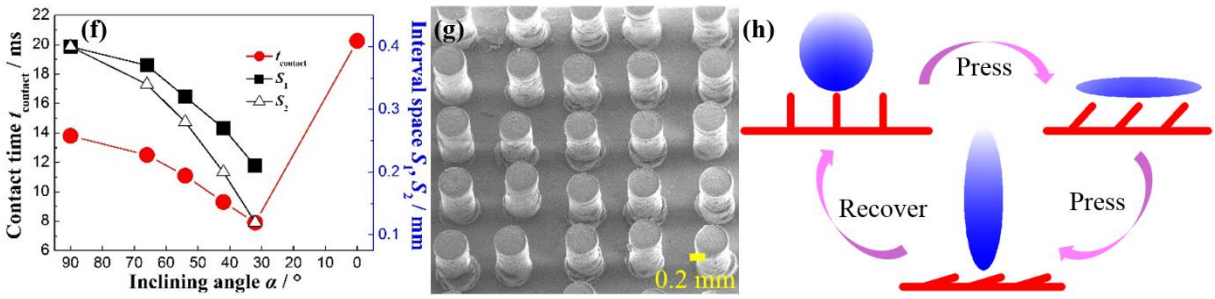

Figure 7. Controlling the contact time and bouncing shape by adjusting the inclination angles of the pillars. (a) Schematic of the inclined pillars. (b) Bouncing shape of a water droplet (17.9 μL, r_0 = 1.62) at the detachment moment on the superhydrophobic pillar arrays with different inclination angles. (c)-(e) SEM images of the superhydrophobic pillar arrays with different inclination angles. (f) The variation of the contact time $t_{contact}$, space S_1 and S_2 with the inclination angles. (g) The inclined SMP pillars were recovered into the straight pillars by heating. (h) Schematics of the reversible switching of bouncing shape and contact time. The dimension of the straight pillars are D = 0.4 mm, H = 1 mm, S = 0.4 mm, and α = 90°. The Webber number We = 13.3.

CONCLUSION

In summary, we have systemically studied the influence of dimension of the superhydrophobic pillar arrays on the contact time and bouncing shape of impacting water droplets. It is revealed that the contact time was affected by space, pillar diameter, and pillar height. For water droplet with volume of 17.9 μL, when the space ≤ 0.25 mm, pillar diameter ≤ 1.25 mm, and pillar heights between 0.6 to 1.0 mm, the pancake bouncing phenomenon was observed, that is pancake bouncing is present on the superhydrophobic pillar arrays with diameter > 1 mm and height-diameter-ratio < 1. We also studied the influence of We on the contact time. When the pillar diameter ≤ 1.05 mm, pancake bouncing can be obtained over a larger region of We which

is ≥ 5.5. Then, we developed a simple replication-spraying method to large-area fabricate the superhydrophobic pillar arrays for pancake bouncing. Since the height-diameter-ratio of the pillars was smaller than 1 and the diameter of the pillars was larger than 1 mm, the pillars were easily replicated and lifted off completely from the mold without the use of a sacrificial layer and any damage to the mold. Since the contact time was rather sensitive to the space between the pillars, based on the special memory ability of the shape memory polymer, we realized that the control of the contact time, bouncing shape, horizontal bouncing direction and reversible switch between pancake bouncing and conventional bouncing by reversibly adjusting the inclination angle of the pillars. This work resolved the problem that the pancake bouncing surface is difficult to achieve over large-area fabrication. This will promote the practical applications of the pancake bouncing surface.

EXPERIMENTAL SECTION

Fabrication of superhydrophobic pillar arrays for dimension optimization

The through hole arrays with different diameter and space were first drilled on the Al plate with a thickness of 1 mm by a precision micro-drilling-milling machine to form an Al mold which was then washed with 0.4 mol/L aqueous hydrochloric acid solution followed by rinsing with deionized water. The pre-polymer of the shape memory polymer (SMP) was formed by mixing bisphenol A diglycidylether (Alighting co., Shanghai), n-octylamine (Alighting co., Shanghai), and m-xylylenediamine (Alighting co., Shanghai) in a mass ratio of 4:2:1 which was poured onto the Al mold with the downside covered with a plastic plate. This was baked at 60 ºC for 2 h followed by 100 ºC for 1 h. Then, the Al mold filled polymer was immersed in the 4 mol/L aqueous hydrochloric acid solution to dissolve the Al and obtain the pillar arrays. The pillar arrays were rinsed with deionized water and dried. Then, the whole polymer sample was

treated using a commercial spray (*Never Wet*) consisting of hydrophobic nanoparticles dispersed in acetone. After solvent evaporation, the superhydrophobic pillar arrays were obtained. The schematics of the fabrication processes are shown in Figure S8.

Characterization

The morphologies of the samples were characterized using a scanning electron microscope (SEM, JSM-6360LV, Japan) at an accelerating voltage of 10 kV. The wettability was characterized using an optical contact angle meter (Krüss, DSA100, Germany) by measuring the advancing, receding and apparent contact angles of water droplets with volume of 10 μL at ambient temperature.[34,35] Advancing, apparent, and receding angles were 165°±3°, 162°±1°, and 158°±3°. The dynamic bouncing processes of water droplets on the superhydrophobic pillar arrays were studied using a Phantom Fastcam SA5 high-speed camera (8000 frame/s). Water droplets with volume of 17.9 μL were dropped from a height of 30 mm (tip to surface) using a micro-syringe at ambient temperature. Pancake bouncing was defined as the ratio (Q) of the lateral extension diameter of water droplet when it detaches from the surface (d_{jump}) and the maximum lateral extension diameter of water droplet in the jumping processes (d_{max}) larger than 0.8, that is $Q = (d_{jump}/d_{max}) > 0.8$,[21,36] as shown in Figure S9. The Weber number We is defined as $We = \rho v^2 r_0/\gamma$, where ρ, v, r_0, and γ relate to the density, impact velocity, radius and surface tension of water droplet, respectively.

ASSOCIATED CONTENT

Supporting Information

Videos of bouncing of droplets. This material is available free of charge *via* the Internet at http://pubs.acs.org.

AUTHOR INFORMATION

Corresponding Author

*Email: xinliu@dlut.edu.cn.

Author Contributions

The manuscript was written through contributions of all authors. All authors have given approval to the final version of the manuscript.

ACKNOWLEDGMENTS

This project was financially supported by National Natural Science Foundation of China (NSFC, 51605078), Science Fund for Creative Research Groups of NSFC (51621064), National Basic Research Program of China (2015CB057304), and the Fundamental Research Funds for the Central Universities (DUT17JC25). Y. Lu acknowledges the support from EPSRC project EP/N024915/1.

REFERENCES

[1] Bergeron, V.; Bonn, D.; Martin, J. Y.; Vovelle, L. Controlling Droplet Deposition with Polymer Additives. *Nature* **2000**, *405*, 772-775.

[2] Tuteja, A.; Choi, W.; Ma, M.; Mabry, J. M.; Mazzella, S. A.; Rutledge G. C.; McKinley G. H.; Cohen R. E. Designing Superoleophobic Surfaces. *Science* **2007**, *318*, 1618-1622.

[3] Deng, X.; Mammen, L.; Butt, H.; Vollmer, D. Candle Soot as a Template for a Transparent Robust Superamphiphobic Coating. *Science* **2012**, *335*, 67-70.

[4] Mishchenko, L.; Hatton, B.; Bahadur, V.; Taylor, J. A.; Krupenkin, T.; Aizenberg, J. Design of Ice-free Nanostructured Surfaces Based on Repulsion of Impacting Water Droplets. *ACS Nano* **2010**, *4*, 7699-7707.

[5] Kim, J.; Rothstein, J. P. Droplet Impact Dynamics on Lubricant-Infused Superhydrophobic Surfaces: The Role of Viscosity Ratio. *Langmuir* **2016**, *32*, 10166-10176.

[6] Farhangi, M. M.; Graham, P. J., Choudhury N. R.; Dolatabadi A. Induced Detachment of Coalescing Droplets on Superhydrophobic Surfaces. *Langmuir* **2012**, *28*, 1290-1303.

[7] Merlen, A.; Brunet, P. Impact of Drops on Non-wetting Biomimetic Surfaces. *J. Bionic Eng.* **2009**, 6, 330-334.

[8] Deng, T.; Varanasi, K. K.; Hsu, M.; Bhate, N.; Keimel, C.; Stein, J.; Blohm, M. Nonwetting of Impinging Droplets on Textured Surfaces. *Appl. Phys. Lett.* **2009**, *94*, 13310913.

[9] Jung, Y.; Bhushan, B. Dynamic Effects of Bouncing Water Droplets on Superhydrophobic Surfaces. *Langmuir* **2008**, *24*, 6262-6269.

[10] Clanet, C.; Beguin, C.; Richard, D.; Quere, D. Maximal Deformation of An Impacting Drop. *J. Fluid Mech.* **2004**, *517*, 199-208.

[11] Liu, X.; Cheng, P.; Quan, X. Lattice Boltzmann Simulations for Self-Propelled Jumping of Droplets after Coalescence on A Superhydrophobic Surface. *Int. J. Heat Mass Tran.* **2014**, *73*, 195-200.

[12] Vasileiou, T.; Gerber, J.; Prautzsch, J.; Schutzius, T. M.; Poulikakos, D. Superhydrophobicity Enhancement Through Substrate Flexibility. *P. Natl. Acad. Sci. U. S. A.* **2016**, *113*, 13307-13312.

[13] Weisensee, P. B.; Tian, J.; Miljkovic, N.; King, W. P. Water Droplet Impact on Elastic Superhydrophobic Surfaces. *Sci. Rep.* **2016**, *6*, 30328.

[14] Song, M.; Ju J.; Luo, S.; Han, Y.; Dong, Z.; Wang, Y.; Gu, Z.; Zhang, L.; Hao, R.; Jiang, L. Controlling Liquid Splash on Superhydrophobic Surfaces by a Vesicle Surfactant. *Science Adv.* **2017**, *3*, 3.

[15] Damak, M.; Mahmoudi, S. R.; Hyder, M. N.; Varanasi, K. K. Enhancing Droplet Deposition through In-Situ Precipitation. *Nat. Commun.* **2016**, *7*, 12560.

[16] Yeong, Y.; Burton, J.; Loth, E.; Bayer, I. S. Drop Impact and Rebound Dynamics on An Inclined Superhydrophobic Surface. *Langmuir* **2014**, *30*, 12027-12038.

[17] Richard, D.; Clanet, C.; Quere, D. Surface Phenomena - Contact Time of A Bouncing Drop. *Nature* **2002**, *417*, 811.

[18] Bird, J. C.; Dhiman, R.; Kwon, H.; Varanasi, K. K. Reducing The Contact Time of A Bouncing Drop. *Nature* **2014**, *505*, 7483.

[19] Gauthier, A.; Symon, S.; Clanet, C.; Quere, D. Water Impacting on Superhydrophobic Macrotextures. *Nat. Commun.* **2015**, *6*, 8001.

[20] Liu, Y.; Andrew, M.; Li, J.; Yeomans, J. M., Wang, Z. Symmetry Breaking in Drop Bouncing on Curved Surfaces. *Nat. Commun.* **2015**, *6*, 10034.

[21] Liu, Y.; Moevius, L.; Xu, X.; Qian, T.; Yeomans, J. M.; Wang, Z. Pancake Bouncing on Superhydrophobic Surfaces. *Nat. Phys.* **2014**, *10*, 515-519.

[22] Liu, Y.; Whyman, G.; Bormashenko, E.; Hao, C.; Wang, Z. Controlling Drop Bouncing using Surfaces with Gradient Features. *Appl. Phys. Lett.* **2015**, *107*, 0516045.

[23] Liu, Y.; Wang, Z. Superhydrophobic Porous Networks for Enhanced Droplet Shedding. *Sci. Rep.* **2016**, *6*, 33817.

[24] McDonald, B.; Shahsavan, H.; Zhao, B. Biomimetic Micro-Patterning of Epoxy Coatings for Enhanced Surface Hydrophobicity and Low Friction. *Macromol. Mater. Eng.* **2014**, *299*, 237-247.

[25] Yuan, L.; Wu, T.; Zhang, W.; Ling, S.; Xiang, R.; Gui, X.; Zhu, Y.; Tang, Z. Engineering Superlyophobic Surfaces on Curable Materials Based on Facile and Inexpensive Microfabrication. *J. Mater. Chem. A* **2014**, *2*, 6952-6959.

[26] Choi, H.; Choo, S.; Shin, J.; Kim, K.; Lee, H. Fabrication of Superhydrophobic and Oleophobic Surfaces with Overhang Structure by Reverse Nanoimprint Lithography. *J. Phys. Chem. C* **2013,** *117*, 24354-24359.

[27] Jiang, T.; Koch, J.; Unger, C.; Fadeeva, E.; Koroleva, A.; Zhao, Q.; Chichkov B. Ultrashort Picosecond Laser Processing of Micro-Molds for Fabricating Plastic Parts with Superhydrophobic Surfaces. *Appl. Phys. A-Mater.* **2012**, *108*, 863-869.

[28] Su, C.; Xu, Y.; Gong, F.; Wang, F.; Li, C. The Abrasion Resistance of A Superhydrophobic Surface Comprised of Polyurethane Elastomer. *Soft Matter* **2010**, *6*, 6068-6071.

[29] Liu, X.; Wu, W.; Wang, X.; Luo, Z.; Liang, Y.; Zhou, F. A Replication Strategy for Complex Micro/nanostructures with Superhydrophobicity and Superoleophobicity and High Contrast Adhesion. *Soft Matter* **2009**, *5*, 3097-3105.

[30] Yarin, A. L. Droplet Impact Dynamics: Splashing, Spreading, Receding, Bouncing. *Annu. Rev. Fluid Mech.* **2006**, *38*, 159.

[31] Rioboo, R.; Marengo, M.; Tropea, C. Time Evolution of Liquid Drop Impact onto Solid, Dry Surfaces. *Exp. Fluids* **2002**, *33*, 112-124.

[32] Lv, T.; Cheng, Z.; Zhang, D.; Zhang, E.; Zhao, Q.; Liu, Y.Y., Jiang, L. Superhydrophobic Surface With Shape Memory Micro/Nanostructure and Its Application in Rewritable Chip for Droplet Storage. *ACS Nano* **2016**, *10*, 9379-9386.

[33] Wang, W.; Salazar, J.; Vahabi, H.; Joshi-Imre, A.; Voit, W. E.; Kota, A. K. Metamorphic Superomniphobic Surfaces. *Adv. Mater.* **2017**.

[34] Marmur, A.; Claudio, D. V.; Stefano, S.; Alidad, A.; Drelich, J. W. Contact Angles and Wettability: Towards Common and Accurate Terminology. *Surf. Innov.* **2017**, *5*, 3-8.

[35] Marmur, A. A Guide to The Equilibrium Contact Angles Maze. In *Contact Angle, Wettability and Adhesion*; Mittal, K. L., Eds.; Brill/VSP: Leiden, 2009; pp 3-18.

[36] Moevius, L.; Liu, Y.; Wang, Z.; Yeomans, J. Pancake Bouncing: Simulations and Theory and Experimental Verification. *Langmuir* **2014**, *30*, 13021-13032.